



Cite this: *Food Funct.*, 2024, **15**, 11115

Immunomodulatory properties of hempseed oligopeptides in an LRRK2-associated Parkinson's disease animal model†

Maria Torrecillas-Lopez, ^{a,c} Fernando Rivero-Pino, ^{†,a,c,e} Paula Trigo, ^b Rocio Toscano-Sanchez, ^a Teresa Gonzalez-de la Rosa, ^{a,c} Alvaro Villanueva, ^d M. Carmen Millan-Linares, ^d Sergio Montserrat-de la Paz ^{*,a,c} and Carmen M. Claro-Cala ^{b,c}

Parkinson's disease (PD) is the second most common neurodegenerative disease, with genetic factors like mutations in the LRRK2 gene being a key cause of late-onset autosomal dominant parkinsonism. Nutritional strategies, such as using bioactive peptides with anti-inflammatory properties from sources like hemp protein, are gaining interest as an alternative to pharmacological therapies. In this study, we used an LRRK2-associated PD mouse model to test the efficacy of a hempseed protein hydrolysate (HPH60A + 15F) with antioxidant and anti-inflammatory properties. Mice were given HPH60A + 15F (10 mg kg⁻¹ day⁻¹) orally for 7 days. After treatment, brain tissue and macrophages were analyzed to assess neuroinflammation markers. Additionally, the neuroavailable peptidome was characterized using an *in vitro* model simulating the intestinal and blood–brain barriers. The oral treatment has been shown to reduce protein aggregates of α-syn, CD68, iNOS, and COX2 in the brain. The treatment also significantly lowered TNF-α gene expression in the striatum, with a notable reduction in the gene expression of other pro-inflammatory cytokines in bone marrow-derived macrophages (BMDMs), such as IL-1β or IL-6. The peptide TVTAMNVVYALK was proposed as a potential highly active peptide, able to exert anti-inflammatory effects in the brain. The results have shown that HPH60A + 15F is capable of alleviating neuroinflammation by reducing the expression of pro-inflammatory cytokines, which could have promising effects in PD.

Received 3rd July 2024,
Accepted 22nd September 2024
DOI: 10.1039/d4fo03167a
rsc.li/food-function

Introduction

The use of bioactive peptides in functional foods is gaining interest in the food industry, as well as in the scientific community, given their advantages of production from natural sources and their high benefits for human health. At the same time, the use of plant proteins in society is increasing, as consumers are aware of the health benefits and the environmentally friendly character that their consumption can have com-

pared to traditional sources of animal origin.^{1,2} One of the promising plant sources whose investigation has been increasing recently is hemp protein. Hempseeds have been demonstrated to be a sustainable source of high-quality protein, including globulin (edestin) which accounts for 60–80%, and albumin, which constitutes the rest.³ The potential health benefits that its consumption might have on different markers have been recently reviewed, and some human studies have demonstrated positive effects on glycemic control, hindgut

^aDepartment of Medical Biochemistry, Molecular Biology, and Immunology, School of Medicine, University of Seville, Spain. E-mail: delapaz@us.es; Tel: +34 954 559 850

^bDepartment of Pharmacology, Pediatrics, and Radiology, School of Medicine, Universidad de Sevilla, Av Sanchez Pizjuan s/n, 41009 Seville, Spain

^cInstituto de Biomedicina de Sevilla, IBI/S/Hospital Universitario Virgen del Rocío/CSIC/Universidad de Sevilla, Sevilla, 41013, Spain

^dDepartment of Food and Health, Instituto de la Grasa (IG-CSIC), C\Utrera Km 1, Campus Universitario Pablo de Olavide, Building 46, Seville, 41013, Spain

[†]European Food Safety Authority, Nutrition and Food Innovation Unit, Novel Foods Team, Parma, Italy

Electronic supplementary information (ESI) available. See DOI: <https://doi.org/10.1039/d4fo03167a>

[‡]Disclaimer: The author F. Rivero-Pino is carrying out a temporal secondment at European Food Safety Authority – EFSA – from June 1, 2024, to May 31, 2025. The work described in this article is not related to his current work at EFSA, it is published under the sole responsibility of the author and may not be considered as an EFSA scientific output. The views and opinions expressed in this manuscript do not represent those of EFSA.

function, and antioxidant status.^{4–6} On top of that, the use of food-grade proteases to produce hempseed protein hydrolysates (HPHs) from protein concentrates or isolates is gaining interest to manufacture a pool of oligopeptides in which some of them might exert certain bioactivity and could be used to promote health in humans.⁷ In this regard, our research group has widely explored the antioxidant⁸ and anti-inflammatory properties, as well as the bioavailability^{9,10} of several protein hydrolysates obtained with alcalase and flavourzyme, and the results have shown that a hydrolysate obtained by subjecting the hemp protein isolate (HPI) to 60 min of hydrolysis with alcalase, followed by 15 min with flavourzyme (HPH60A + 15F) exerts high activity in murine microglia¹¹ and in primary human monocytes.¹² Considering all these *in vitro* results, we hypothesize that HPH60A + 15F could have neuromodulatory effects *in vivo*, and these assays could be used to explain the underlying mechanisms if improvements in neurological parameters are found.

On the other hand, Parkinson's disease (PD) is the second most common neurodegenerative disease and is associated with a loss of nigrostriatal dopaminergic innervation in the substantia nigra pars compacta (SNpc) area. Although its cause is unknown, several genetic and environmental predisposing factors have been characterized. One of these is the Leucine-Rich Repeat Kinase 2 (LRRK2) gene, whose mutations are the most prevalent cause of late-onset autosomal dominant parkinsonism.¹³ The most common mutation G2019S is found in up to 40% of patients in certain ethnic populations. In addition to pathogenic mutations, common genetic variability in LRRK2 is a risk factor for sporadic PD.^{14,15} Specifically, cell death in the SNpc is restricted to a group of neuromelanin-containing dopaminergic neurons called A9 neurons. Dopaminergic neuronal loss is accompanied by intraneuronal inclusions known as Lewy bodies,¹⁶ which are protein aggregates that are cytoplasmically deposited within neuronal cell bodies and are immunoreactive to the protein α -synuclein (α -syn). The α -syn protein in a healthy brain is found without a defined tertiary structure or forming α -helical structures, while in a brain with PD, this protein adopts an amyloid-like structure that is fibrils rich in β -sheets, tending to form aggregates. The LRRK2 protein is also involved in the aggregation of α -syn. Studies in transgenic mice have shown that LRRK2-G2019S mutations increase α -syn aggregation, leading to an increase in associated neuroinflammatory and behavioral alterations.¹⁷ On the other hand, neuroinflammation is a tissue response of the cells of the central nervous system (CNS) to an alteration of tissue homeostasis and neuronal damage. Neuroinflammation generated in microglia and astrocytes is a feature of PD.¹⁸ This is because microglia produce factors that can be potentially neurotoxic, such as pro-inflammatory cytokines (tumor necrosis factor-alpha (TNF- α) and interleukin-1 β (IL-1 β)), nitric oxide (NO), and reactive oxygen species (ROS). In addition, it has been shown that individuals with polymorphisms in the TNF- α and IL-1 β genes suffer an increased risk of developing PD.¹⁹

Due to the lack of a treatment that cures PD, there are currently open lines of research with several novel and promising

approaches, including both the study of new experimental compounds and the reuse of drugs or the use of bioactive peptides, since, as mentioned above, their anti-inflammatory properties have been demonstrated *in vitro*. However, *in vivo* studies are lacking to demonstrate the efficacy of these food-derived protein hydrolysates containing bioactive oligopeptides.²⁰ Considering that the blood-brain barrier (BBB) is the primary barrier with a highly selective semipermeable border between the endothelial cells of blood vessels and the CNS, BBB penetrating peptides are a neurotherapeutic alternative for brain-related disorders, as they can facilitate their delivery to the brain. In this work, we used an LRRK2 murine model, where inflammation is responsible for neurodegeneration, to evaluate the neuroprotective effect of HPH60A + 15F. For this purpose, protein expression and gene expression with parameters related to PD development were evaluated after a treatment of 7 days of administrating the hydrolysate. In addition, the neuroavailable peptidome collected by cell culture was identified and characterized by *in silico* analyses including prediction tools and molecular docking.

Materials and methods

Chemicals and samples

Cannabis sativa L. seeds were provided by Sensi Seeds Bank (<https://sensiseeds.com/>). The proteases employed to produce HPH60A + 15F, alcalase 2.4 L and flavourzyme 1000 L were provided by Novozymes (Bagsvaerd, Denmark). The rest of the reagents and solvents employed were of analytical grade and purchased from Sigma Chemical Co., Bachem AG (Bubendorf, CH, EU), and Gibco (Waltham, MA, USA).

Preparation and chemical characterization of the hemp protein hydrolysate

The HPH was obtained by subjecting an HPI to enzymatic hydrolysis with alcalase and flavourzyme. According to the antioxidant and anti-inflammatory activities of a series of HPHs measured *in vitro*, the sample was obtained by subjecting the protein to hydrolysis by alcalase for 60 min, followed by 15 min with flavourzyme (*i.e.*, HPH60A + 15F). Details on the process to obtain the HPH and its characterization can be found elsewhere Montserrat-de la Paz *et al.* (2023).^{9,10} The chemical characterization of the HPH included analysis of protein, total fiber, ash, phenols, and sugars. In addition, the amino acid content was evaluated and peptidome was analyzed, including *in silico* analysis. A detailed description of the methodology and results can be found in previous works.⁸ Briefly, HPH60A + 15F contained 82.3% of protein, with a high content of amino acids such as glutamic acid, aspartic acid, arginine, phenylalanine, and tyrosine. The complete characterization can be found in ESI – Tables 1 and 2.†

Experimental animal model and study design

Male LRRK2-G2019S KI mice were provided by the Institute of Biomedicine of Seville and kept in the animal facility of the



Faculty of Medicine of the University of Seville (registration code: 202399903491663). The protocol for animal handling and experimentation was in agreement with the European Union Community guidelines for the ethical treatment of animals (EU Directive of 2010; 2010/63/EU) and was approved by the Ethics Committee for Animal Research of the University of Seville (RD 53/2013). The housing conditions were as follows: the temperature was constant (21 ± 2 °C) and the light–dark cycle was of 12 hours. The animals were randomly assigned ($n = 10\text{--}12$) at 18 months of age and the acute treatment consisted of daily administration by an esophageal catheter of a dose of 10 mg of HPH60A + 15F per kilogram of animal (final volume 100 µL) for 7 days. For the control group of animals, in which no treatment was provided, mineral water (final volume 100 µL) was administered. After the seventh day of treatment, mice were sacrificed, previously anaesthetized by intraperitoneal injection of ketamine (100 mg per kg of animal) and xylazine (5 mg per kg of animal). A sample of fresh brain tissue was removed and dissected, separating the cortex and striatum according to the reference anatomical atlas,²¹ then immediately frozen and stored at -80 °C until further analysis for subsequent RT-qPCR studies. Bone marrow (BM) cells were also extracted for subsequent RT-qPCR studies. Furthermore, the animals were perfused for studies using the immunohistochemistry (IHC) technique.

Determination of protein expression by immunohistochemistry

The animals were perfused through the heart under deep anesthesia with 4% paraformaldehyde in phosphate buffer, pH 7.4. The brains were then removed and then immersed in sucrose in PBS, pH 7.4, first in 10% sucrose for 24 h and then in 30% sucrose until they sank (2–5 days). The tissues were then frozen in isopentane, and sections were cut on a cryostat (Leica CM1950 cryostat; Heidelberg, Germany). The identification of the different areas of the brain was carried out according to the anatomical atlas of the mouse brain.²¹ The brains were sectioned to a thickness of 20 µm and collected in a 24-well plate filled with 0.1 M PBS. Sections were washed in PBS for 10 min, treated with 0.3% hydrogen peroxide in methanol, and pre-incubated in 10% normal goat serum for 1 h. The sections were then incubated overnight at 4 °C with primary antibody α -syn (1 : 200; Santa Cruz Biotech, Heidelberg, Germany), iNOS (1 : 200; Santa Cruz Biotech, Heidelberg, Germany), CD68 (1 : 100 Bio-Rad, Madrid, Spain), and COX2 (1 : 200; Santa Cruz Biotech, Heidelberg, Germany). These plates were stored at 4 °C until use. An ABC kit was used and a diaminobenzidine (DAB) solution was prepared to reveal the immunohistochemical sections. The revealed sections were mounted on gelatinized slides, following the neuroanatomical order. The analysis of the results was carried out after capturing photographs using the Olympus XM10 monochrome cold light digital camera which was placed in the Olympus BX41 optical microscope and connected to a computer with imaging software (Olympus cell^{^F}).

Extraction and culture of murine bone marrow cells and differentiation to macrophages

BM cells were isolated and pooled for each group of mice. The femora and tibiae were septically removed and dissected to free them from the adherent soft tissue. The bone ends were cut, and the marrow cavity was flushed into a Petri dish by slowly injecting ice-cold PBS solution at one end of the bone using a sterile 21-gauge needle. The BM cell suspension was carefully agitated with a plastic Pasteur pipette to obtain a single cell suspension. The cells were washed and depleted of red blood cells using hypotonic lysis buffer. After washing twice with PBS, the cells were cultured and differentiated into BM-derived macrophages (BMDMs) for 6 days at 37 °C under a humidified atmosphere containing 5% CO₂ in 12-well plates containing RPMI 1640 medium plus 10% heat inactivated fetal bovine serum (FBS), 1% penicillin G/streptomycin (P/S), and 20 ng mL⁻¹ murine M-CSF (Peprotech, Madrid, Spain).²² In addition, BMDMs from the animals were exposed to LPS (100 ng mL⁻¹) for an additional 24 h to generate 4 groups of cells: C (control, no treatment), C + LPS, HPH60A + 15F, and HPH60A + 15F + LPS. On day 7, the cells were collected.

RT-qPCR analysis of fresh tissue from the striatum and BMDMs

To extract genetic material from the brain, in this case caudate and putamen, the tissue was placed on a filter on top of a 50 mL tube and disintegrated with PBS, which aids in disintegration with pressure and agitation with the plunger of a syringe. Once the entire tissue was disintegrated, the tissue suspension obtained was centrifuged, and the supernatant was removed. Total RNA was extracted using TRIzol Reagent (Bioline, Meridian Life Science, Inc., Memphis, USA). RNA quality was assessed by the A_{260}/A_{280} ratio in a NanoDrop ND-2000 (ThermoFisher Scientific, Madrid, Spain). Briefly, RNA (250 ng) was subjected to reverse transcription (iScript, Bio-Rad, Madrid, Spain). Between 10 and 30 ng of cDNA were used as a template for RT-qPCR amplifications. mRNA levels for specific genes were determined using the CFX96 (Bio-Rad) system. For each PCR reaction, an optimal volume of the cDNA template was added, containing the primer pairs for either gene or glyceraldehyde 3-phosphate dehydrogenase (GAPDH) as the constitutive gene. Quantitative PCR was performed using Bio-Rad's iTaqTM Universal SYBR[®] Green Supermix. The relative mRNA expression of candidate genes was calculated using the mean threshold cycle (C_t) numbers of the samples. The magnitude of the change in mRNA expression for candidate genes was calculated using the standard method $2^{-(\Delta\Delta C_t)}$. All data were normalized with respect to endogenous reference gene content and expressed as relative control values. The sequences of the designed oligonucleotides are shown in the ESI – Table 3.†

Statistical analysis

All RT-qPCR data are expressed as arithmetic means \pm standard deviations (SD). The values were estimated using version

8.01 of GraphPad Prism software (San Diego, CA, USA). To IHC and gene expression in brain tissue, an unpaired *t*-test for equality of variances was used. For gene expression in BMDMs, the statistical significance of the variances between the groups was analyzed using a one-way ANOVA, following Bonferroni's multiple comparison test as a *post hoc* test. Any *P* value less than 0.05 was considered statistically relevant.

Central nervous system availability assay using a transwell system

To study the availability of the HPH60A + 15F in the brain, a double *transwell* system was used. HPH60A + 15F was applied to the apical area of the system using Caco-2 cells as the first model of the intestinal barrier. The bioavailable hydrolysate (bioHPH60A + 15F) is collected in PBS in the basolateral zone. This bioHPH60A + 15F is then transferred to a second *transwell* system composed of epithelial brain microvascular endothelial cells (HBEC-5i) and the neuroavailable hydrolysate (neuroHPH60A + 15F) corresponds to the sample collected in this case. Both cell lines were cultured in 12-well cell culture inserts in DMEM medium supplemented with 10% heat-inactivated FBS and 1% P/S. The cells were incubated at 37 °C in a 5% CO₂ modified atmosphere and fed fresh medium every 2–3 days. The integrity of the cell monolayer was controlled by transepithelial electrical resistance using a Millicell® ERS-2 (Millipore) voltammeter perimeter. The inserts were used for 1–2 weeks after plating and had a resistance of at least 500 Ω cm⁻².

Neuroavailable peptidome identification, *in silico* analysis, and molecular docking

Identification of neuroavailable peptides. Samples were acidified with 0.5% trifluoroacetic acid. The desalination and concentration steps were performed with ZipTip C18 (Millipore) and were vacuum dried. Liquid nanochromatography coupled to high-performance tandem mass spectrometry with ion mobility (LC-TIMS-MS/MS) was carried out using the Elute nanoflux UHPLC (Bruker Daltonics, Bremen, Germany), coupled to a TIMS-TOF Pro 2 mass spectrometer, equipped with a CaptiveSpray nanoelectrospray ion source (Bruker Daltonics) according to the procedure described in Montserrat de la Paz *et al.* (2023).¹⁰

In silico analyses of neuroavailable peptides. The neuroavailable peptidome was subsequently subjected to *in silico* analyses: (a) ToxinPred software was used to predict hydrophobicity, steric hindrance, solubility, isoelectric point (pI) charge, and amphipathicity²³ for each peptide. (b) The PASTA 2.0 server was obtained to estimate the type of secondary structure that the peptide (<https://old.protein.bio.unipd.it/pasta2/>) would present. (c) AnOxPePred-1.0 was used to predict the antioxidant properties (quantified by free radical scavenging (FRS) and ion chelation scores (CHEL) of peptides.²⁴ (d) The PreAIP tool was used to estimate the probability that the peptide has anti-inflammatory properties.²⁵ (e) The preTP-Stack tool allows the calculation of the probability of a peptide being considered anti-inflammatory.²⁶ (f) SCMB3PP

was used to predict whether the peptide could penetrate the BBB.²⁷ (g) PeptideRanker was used to estimate the likelihood of each peptide being bioactive.²⁸

Molecular docking of neuroavailable peptide selected.

Molecular docking was carried out to determine the binding affinity energy of the neuroavailable peptide TVTAMNVVYALK with the receptors α-syn (PDB: 1XQ8), catechol-O-methyltransferase (COMT; PDB: 3A7E), and monoamine oxidase-B (MAO-B; PDB: 2V5Z). The X-ray crystal structures of these receptors were obtained from the RCSB PDB database (Protein Data Bank, <https://www.rcsb.org/>). Ligands and all the water molecules were removed from the receptor PDB file, while polar hydrogen atoms were added using UCSF Chimera software. The 3D structure of the peptide TVTAMNVVYALK was obtained, and its structure was minimized by UCSF Chimera. Then, the molecular structures of the receptors and the peptide were converted to PDBQT format with AutoDock Tools. The AGFR program was used to calculate the positions and sizes of the specific docking boxes for each receptor in their active site. Finally, the potential best docking score determined was selected and visualized *via* Biovia Discovery Studio Visualizer, as well as the 2-dimensional (2D) and surface annotation of both ligand interactions with the protein.

Results and discussion

Protein expression of α-syn, CD68, iNOS, and COX2 by immunohistochemistry

Using the IHC technique, the protein expression of α-syn, CD68, inducible nitric oxide synthase (iNOS), and cyclooxygenase type 2 (COX2) was determined in the striatum of the brains of LRRK2 mice treated with HPH60A + 15F (LRRK2-HPH) and compared to those that received mineral water as a control (LRRK2-Ct). Fig. 1 for α-syn (Fig. 1A), CD68 (Fig. 1B), iNOS (Fig. 1C), and COX2 (Fig. 1D) shows the different results obtained. Progressive aggregation of the α-syn protein in the substantia nigra of the striatum is a key histopathological hallmark of PD. It has been described that α-syn pathology may spread through neural circuits in the brain, contributing to disease progression. Therefore, it is therapeutically pertinent to identify possible modifications of α-syn aggregation as a potential target to slow down the neurodegeneration of the disease. It has been reported that the aggregation of α-syn increased in primary neurons of mice that expressed the LRRK2 mutation linked to PD by the formation of intracellular protein aggregates in neurons called Lewy bodies, whose main component is this protein, α-syn.¹⁷ Regarding the effects of HPH60A + 15F in relation to the primary antibody α-syn, Fig. 1A also shows the location of the striatum in the coronal sections next to other adjacent structures. As shown by the positive labeling of the diaminobenzidine precipitates, significant differences (*p* = 0.0006) were observed between brain tissue samples from untreated mice (LRRK2-Ct) and those treated for one week with HPH60A + 15F (LRRK2-HPH). In addition, it is important to note that age is a crucial factor for microglial phagocytosis, as



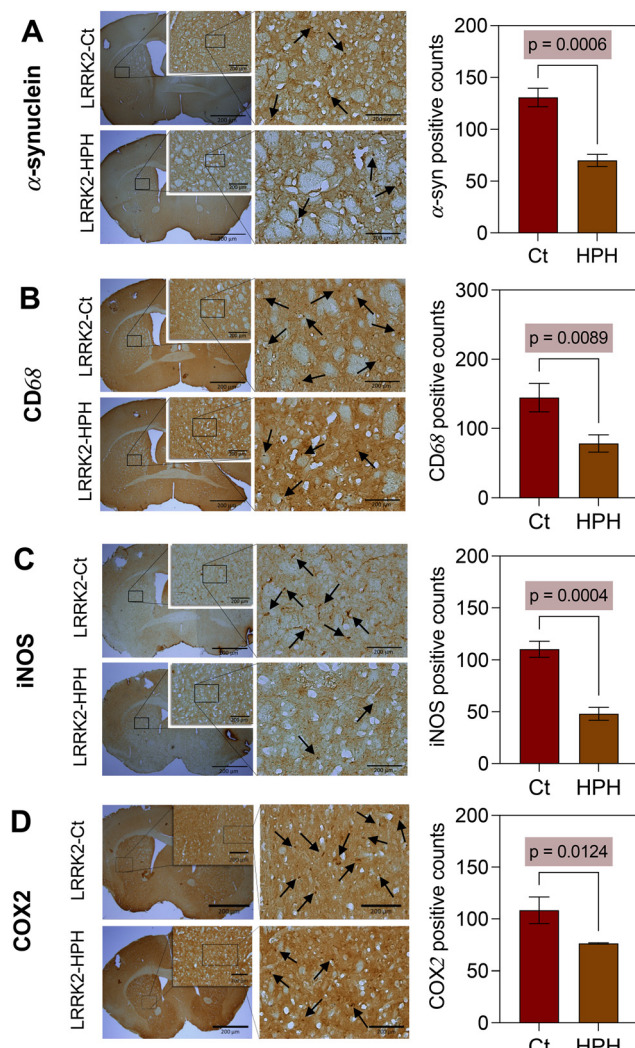


Fig. 1 Stained histological section (scale bar: 200 μm) and quantification of (A) α -synuclein, (B) CD68, (C) iNOS, and (D) COX2 positive cells in the putamen-caudate area of the brain tissue from male LRRK2 mice subjected to daily administration by an esophageal catheter of a dose of water (LRRK2-Ct, red bars) and HPH60A + 15F (10 mg kg^{-1} day $^{-1}$, brown bars) for 7 days. Values are presented as means \pm SD ($n = 6$). Statistical significance was analyzed using an unpaired *t*-test, representing significant *p*-values.

microglia from adult mice were less efficient at phagocytosing oligomeric α -syn than those from young mice, while also responding with increased TNF- α release.³⁰ In this line, using a *Caenorhabditis elegans* PD model, a dietary supplementation (12.5 $\mu\text{g mL}^{-1}$) with peptides from sesame cake led to a reduction in ROS levels and a decrease in α -syn aggregation with an improvement in PD-related pathologies,³⁰ indicating the promising therapeutic effects of seeds-derived peptides in neurological diseases prevention.

On the other hand, previous research has found microglia-derived macrophages in the substantia nigra of PD brains. Activated microglia have been associated with various components of the immune system, including complement recep-

tors and major histocompatibility complex class II (MHCII), and are associated with a wide variety of neurological lesions.³¹ In PD, microglia maintain an uncontrolled pro-inflammatory phenotype, favoring the progression of neurodegeneration. In addition, several studies have suggested that microglia can dynamically change their phenotype in PD depending on the stage of the disease, which may explain the coexistence of both pro-inflammatory and anti-inflammatory molecules in PD.²⁹

Several studies have described the impaired phagocytic function of microglia in PD, although few have focused on the immunohistochemical evaluation of CD68, a macrophage protein and potential marker of phagocytosis. These studies have observed an increase in CD68 expression in PD development (Janda *et al.*, 2018),²⁹ although further research is needed to fully understand its role in PD. Fig. 1B shows the results of IHC performed with the primary antibody against CD68, a glycoprotein expressed in the plasma membrane of macrophages, among other cell types, whose expression can be significantly increased in inflammatory processes.³² The figure shows the tissue from both control and treated groups, where a significant differential protein expression was observed ($p = 0.0089$). Similar to the results obtained in this study, an enzymatically derived sunflower protein hydrolysate and peptides were reported to promote monocyte differentiation to a dendritic cell phenotype through the induced expression of surface markers CD14 and CD86, although these results are limited to *in vitro* studies.³³ Furthermore, numerous previous studies in PD have also investigated cytokines, such as TNF- α and IL-1 β , and enzymes, such as iNOS, COX-2, and metalloproteinases, for their roles in the proinflammatory response.³⁴ iNOS is responsible for synthesizing nitric oxide (NO), a pro-inflammatory mediator, and is only expressed when cells receive some type of stimulus, such as inflammation, mainly in neurons, macrophages, astrocytes, and microglial cells.^{34–36}

Because the LRRK2 model is associated with inflammation, the expression of iNOS in the CNS of these mice was measured aiming to observe whether the expression of iNOS was significantly reduced ($p = 0.0004$) due to its anti-inflammatory effect and, with it, inflammation, which would be reflected in a decrease in protein aggregates in IHC assays (Fig. 1C) in the area of the striatum. Previous pharmacological studies in experimental models of PD have been based on the use of phytocannabinoids for their antioxidant power, given that oxidative stress is an important feature in the pathogenesis of PD (Cinelli *et al.*, 2020; X. Wang & Michaelis, 2010).^{35,37} Even so, these trials are the first indicative step to support the hypothesis of the anti-inflammatory effect of HPH60A + 15F into the brain. On the other hand, inflammatory processes associated with increased expression of the enzyme COX2 and elevated levels of prostaglandin E2 (PGE2) also lead to neurodegeneration. The COX2 enzyme is responsible for converting arachidonic acid into mediators of inflammation and pain, such as prostaglandins. Unlike COX1 and COX3, COX2 is expressed when there is a pro-inflammatory stimulus and, in the brain, its concentration increases in microglia but not in

astrocytes.^{38,39} COX2, therefore, contributes to the neuroinflammatory environment in LRRK2 models, and consequently, the presence or the absence of COX2 in the brain offers an idea of the anti-inflammatory effect of HPH60A + 15F. The results obtained for COX-2 expression in the LRRK2-Ct group compared to the treated LRRK2-HPH group can be seen in Fig. 1D. Similarly, there was a significant decrease in COX-2 expression between the two groups ($p = 0.0124$), indicating that under the conditions assayed, HPH60A + 15F exerted an effect on the COX2 levels. In this line, the anti-inflammatory effects of a corn protein hydrolysate in cells and in a mouse model of colitis were recently reported by Liang *et al.* (2020).⁴⁰ These authors showed that the bioactive peptides in the hydrolysate inhibited the expression of COX2 and iNOS and reduced the secretion of IL-8 in TNF- α -induced inflammation in Caco-2 cells. On top of other changes, in the animal model, a decrease of the myeloperoxidase activity, and down regulation of the expression of TNF- α , and IL-6 in the colon was shown, related to anti-inflammatory activity as reported also in our PD model, indicating the biological relevance of plant protein hydrolysates in managing inflammation. To the authors' knowledge, little research has been carried out on food-derived protein hydrolysates used as neuroprotective agents in animals, evaluating the parameters hereby reported, hindering the discussion on whether these peptides are more effective than those derived from other sources. However, for instance recently it was reported that a fish hydrolysate supplementation prevents stress-induced dysregulation of hippocampal proteins related to mitochondrial metabolism and the neuronal network in mice,⁴¹ following a supplementation of 300 mg kg^{-1} for 7 days. This highlights the need for the evaluation of effects following dose-response analyses, to observe how the supplementation with bioactive compounds might modulate the physiological status of subjects.

Proinflammatory gene expression in LRRK2 mouse brain tissue

RT-qPCR was used to study the gene expression of pro-inflammatory markers in the striatum area of the brain tissue from LRRK2 mice treated with HPH60A + 15F (LRRK2-HPH) compared to control mice (LRRK2-Ct). Bioactive food ingredients in animal and human models have demonstrated numerous biological properties for brain function and protection, including neuroprotective, anti-inflammatory, and immunomodulatory benefits, decreasing the production of inflammatory cytokines, preserving cerebral circulation during ischemic events, and reducing vascular changes and neuroinflammation.⁴² For instance, elevated levels of pro-inflammatory cytokines such as TNF- α , IL-1 β , and IL-6 have been found in the cerebrospinal fluid, striatum, and medulla of experimental animal models and in the brains of PD patients.⁴³ Fig. 2 shows the gene expression of IL-1 β , IL-6, TNF- α , and iNOS in the striatum of the brains of LRRK2 mice, both for the control group and those treated with HPH60A + 15F. In all cases, a trend towards decreased gene expression was observed in the treated group compared to the control group, with this decrease in gene

expression being lower in the case of IL-1 β and IL-6 and greater in the case of TNF- α and iNOS. However, this difference was only statistically significant in the case of TNF- α ($p = 0.0011$). In the pathology of neurodegenerative diseases, IL-1 β is an essential pro-inflammatory cytokine that induces a rapid pro-inflammatory response. It also plays a critical role in neurodegeneration, induces the production of IL-6, and stimulates iNOS activity in astrocytes. IL-6 plays several roles in neuroinflammation, as well as the stimulation of microglial activation of astrogliosis and the increase of the production of acute-phase proteins. In turn, the expression of iNOS in microglial cells and macrophages results in high levels of nitric oxide and peroxynitrite, which ultimately leads to causing damage to the CNS. As for TNF- α , it plays a vital role in the process of acute phase inflammation and, *a priori*, has a protective effect. However, uncontrolled and prolonged expression can lead to chronic inflammation with detrimental effects, as has been observed in multiple neurodegenerative diseases, such as PD.³⁹

In line with the hereby reported results, Ji *et al.* (2021)⁴⁴ described the neuroprotective effects of a tilapia head protein hydrolysate on scopolamine-induced cognitive impairment in mice, showing that the administration of the hydrolysate (400 mg kg^{-1}) for 56 days significantly improved the cognitive behavior of mice, and normalized the cholinergic system and oxidative stress system of the mouse brain. These authors reported an increase in the number of mature neurons marked by NeuN and a delay in the activation of astrocytes in the hippocampus of mice by histopathological observation, showing beneficial effects potentially in line with our observations. In the same line, Wang *et al.* (2020)⁴⁵ evaluated the inhibitory effects of walnut peptides on neuroinflammation and oxidative stress in LPS-induced cognitive impairment in mice. These authors showed that low molecular weight peptides could improve the oxidative stress and inflammatory response in the brain, leading to alleviation of the memory impairments. Similar results were obtained by Wang *et al.* (2021)⁴⁶ showing that a walnut protein hydrolysate could exert remarkable amelioration of behavioral performance after ingestion of $3.3\text{--}6.6 \text{ g kg}^{-1}$. As discussed above, numerous bioactive compounds are able to offer an anti-inflammatory role through decreasing TNF- α levels,⁴⁷ as the tested hydrolysate does, suggesting that HPH60A + 15F could have a potential anti-inflammatory effect at this level. Higher doses or interventions lasting longer might imply significant changes in the other cytokines evaluated, as studies with other protein sources have demonstrated.

Cytokine gene expression in BMDMs isolated from LRRK2 mice

To determine the potential immunomodulatory effects of HPH60A + 15F on BMDM cells from control (LRRK2-Ct) and treated LRRK2 mice (LRRK2-HPH), the gene expression of pro-inflammatory cytokines (TNF- α , IL-1 β , and IL-6) and the anti-inflammatory cytokine IL-10 was analyzed using RT-qPCR. The results obtained are shown in Fig. 3. When BMDMs were stimulated with LPS, the expression of IL-1 β (Fig. 3A), IL-6



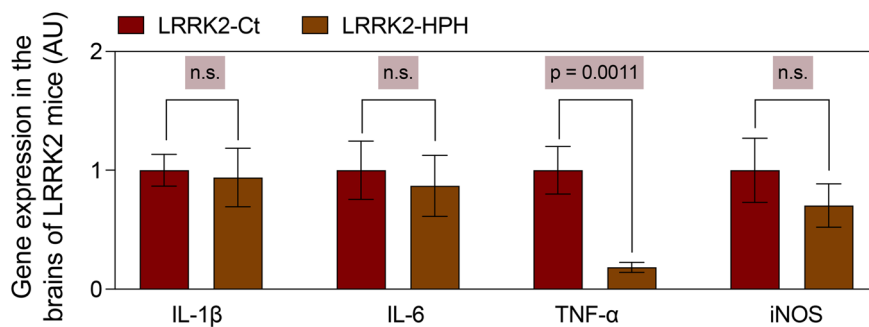


Fig. 2 Relative mRNA levels of IL-1 β , IL-6, TNF- α , and iNOS in the striatum area of the brain tissue from male LRRK2 mice subjected to daily administration by an esophageal catheter of a dose of water (LRRK2-Ct, red bars) and HPH60A + 15F (10 mg kg $^{-1}$ day $^{-1}$, brown bars) for 7 days. Values are presented as means \pm SD ($n = 6$). Statistical significance was analyzed using an unpaired t -test, representing significant p -values.

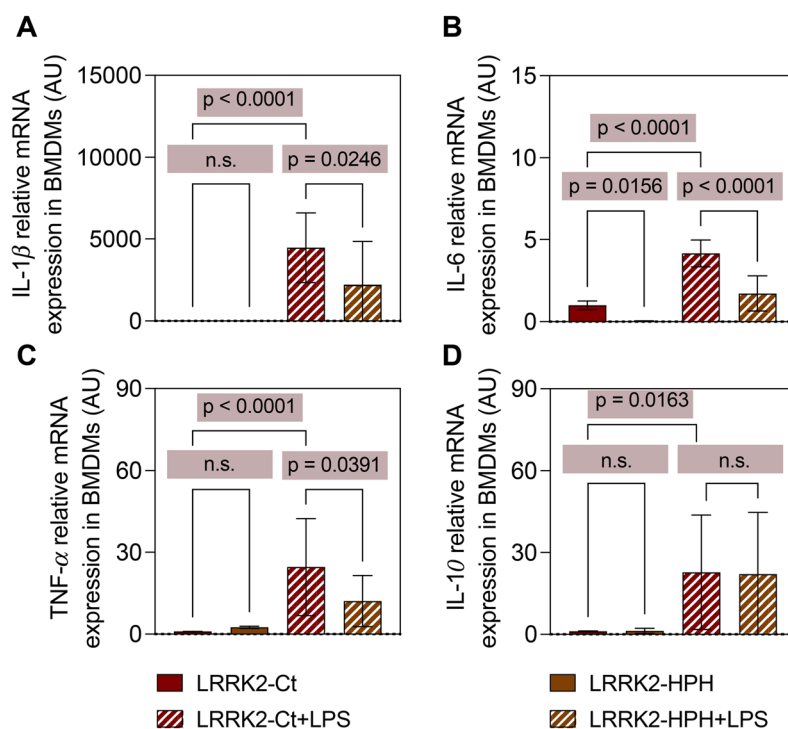


Fig. 3 Relative mRNA levels of (A) IL-1 β , (B) IL-6, (C) TNF- α , and (D) IL-10 in BMDMs from male LRRK2 mice subjected to daily administration of a dose of water (LRRK2-Ct, red bars) and HPH60A + 15F (10 mg kg $^{-1}$ day $^{-1}$, brown bars) with an esophageal catheter for 7 days. BMDMs-LPS (filled bars) were generated as indicated in the Materials and methods section. Values are presented as means \pm SD ($n = 9$). Statistical significance was analyzed using a one-way ANOVA, followed by Bonferroni's multiple comparison test as a *post hoc* test and representing significant p -values.

(Fig. 3B), and TNF- α (Fig. 3C), was significantly increased compared to controls, and mRNA levels were reduced when BMDMs were isolated from mice treated with HPH60A + 15F. These results are consistent with those obtained in previous studies on gene expression following LPS stimulation of BMDMs.⁴⁸ In the case of IL-1 β (Fig. 3A, $p = 0.0246$) and IL-6 (Fig. 3B, $p < 0.0001$), there is a significant decrease in their expression between BMDMs from control mice treated with LPS and BMDMs from HPH60A + 15F-treated mice with LPS. Regarding TNF- α expression (Fig. 3C, $p < 0.0391$), a significant difference was found between its expression in BMDMs from control mice treated with LPS and BMDMs from HPH60A +

15F-treated mice with LPS, showing that the treatment led to a reduction in the expression of this cytokine, and consequently, the administration of HPH60A + 15F led to immunomodulatory effects in the model. Regarding the expression of IL-10, as in previous studies,⁴⁹ it was observed that in BMDMs stimulated with LPS, IL-10 expression increased significantly (Fig. 3D, $p = 0.0163$), showing no significant difference when treated with HPH60A + 15F versus control. As in the previous case with brain tissues, it has been observed that HPH60A + 15F is capable of decreasing the expression of pro-inflammatory cytokines, in this case in BMDMs. Similar results were obtained by Soriano-Romani *et al.* (2022),⁵⁰ who investigated

the immunomodulatory properties of bone collagen peptides on the human monocytic THP-1 cell line, and reported cytokine mRNA expressions in M0 macrophages, especially, a significant increase in the anti-inflammatory IL-10 cytokine biomarker. On top of describing the *in vivo* the benefits of the hydrolysate treatment in the animal model, an approach to investigate the compounds responsible for the activity is the identification of the peptides contained in HPH60A + 15F and those reaching the brain tissue. For this purpose, cell models were used, considering the limitations that quantitative analysis of food-derived peptides in body fluids and tissues shows.⁵¹

Peptidome of neuroHPH60A + 15F and *in silico* prediction of biological activity

The peptidomes of the original HPH60A + 15F, the bioavailable (bioHPH60A + 15F), and the neuroavailable (neuroHPH60A + 15F) at the CNS level were characterized by LC-TIMS-MS/MS. Thus, 1185 peptides were identified in the original HPH60A + 15F,⁸ 554 peptides in the bioHPH60A + 15F,⁹ and 182 peptides in the neuroHPH60A + 15F. In the ESI – Table 4,† the full table of the 182 identified peptides in neuroHPH60A + 15F is shown, together with the outcomes from the *in silico* tools employed. In Table 1, the 20 neuroavailable peptides which ranked the highest in the Pre-AIP tool together with the results from the other *in silico* tools, are depicted. In relation to the physicochemical properties, the hydrophobicity has been correlated with bioactivity, together with low steric hindrance values and high amphipathicity. The ranges of values obtained are highly variable, and consequently, the *in silico* discussion will be mostly based on the specific prediction tools for the whole hydrolysate.

From the neuroHPH60A + 15F, 79 (44%), 75 (41%), 19 (10%), and 9 (5%) sequences out of 182 sequences were considered as high, medium, low, and negative AIP according to Pre-AIP, supporting the *in vivo* activity showed by the peptides, as most of the peptides were considered anti-inflammatory according to the *in silico* tool and only a few of them were categorized as not anti-inflammatory. Similarly, the outcome obtained from the PreTP-Stack tool (assuming the standard threshold of 0.5) showed that 122 sequences could be considered anti-inflammatory therapeutic agents, representing 67% of the neuroHPH60A + 15F, whereas the rest did not. On top of that, in the outcomes from PeptideRanker, 39 sequences had a score higher than 0.5, which is considered the threshold of this tool to hypothesize that a peptide is bioactive, whereas the other sequences did not reach this threshold ($n = 143$). According to this tool, the most bioactive ones (>0.8) would be LPHPAPNFK and VDFLPAAGAFLP, which also showed high values of antioxidant activity related to FRS values and were considered as high and medium anti-inflammatory according to Pre-AIP, respectively.

Regarding the prediction of BBB penetrating peptides, the SCMB3PP tool revealed that 133 peptides would be able to cross this barrier, representing 73% of the sample which was able to cross through the brain microvascular endothelial

cells, which are the main components of this BBB. This result shows that the *in silico* prediction tools are not highly accurate; for example, in this case, 49 sequences were predicted as unable to cross the BBB, whereas the *in vitro* results showed the opposite. However, validation of these results with *in vivo* results is needed.^{51,52} Regarding the antioxidant prediction tool, showing two different scores, for FRS and CHEL, the values were ranging from 0.24 to 0.58 and 0.15 to 0.32, respectively. For the FRS, the most active ones (>0.58) were LNFSHASHEYHAETKL, LNVYYNMPGLE, and AVRPHWNLN, which also had high prediction scores from PreAIP (>0.45) and PreTP (>0.47), indicating that these peptides might be highly contributing to the activity exerted by neuroHPH60A + 15F.

Finally, the contribution of secondary structure to the immunomodulatory and/or anti-inflammatory properties of peptides is yet to be unraveled; however, it must be noted that in the hydrolysate evaluated, 78 peptides were predicted to have 100% coils, with 31 of them predicted to be highly anti-inflammatory according to PreAIP and 57 according to the PreTP Stack tool. This could be an indicative of the properties of peptides having specific bioactivities, although more research and validation with synthetic peptides are required.

TVTAMNVVYALK, a neuroavailable peptide with therapeutic potential identified in neuroHPH60A + 15F. A comparison of all the peptidomes (original HPH60A + 15F, bioHPH60A + 15F, and neuroHPH60A + 15F) showed that only one peptide was presented in the three hydrolysates. The sequence of this 12-amino acid peptide was Threonine–Valine–Threonine–Alanine–Methionine–Asparagine–Valine–Valine–Tyrosine–Alanine–Leucine–Lysine (TVTAMNVVYALK), demonstrating its potential to resist gastrointestinal digestion *in vitro*, reach the systemic circulation and cross the BBB to exert its neuroprotective function. Table 1 shows the physicochemical properties, including molecular weight, net load, pI, hydrophobicity, steric impediment and amphipathicity, and the secondary structure shown using PASTA 2.0.; the antioxidant, anti-inflammatory, therapeutic, and the neuroavailable potential are detailed. In addition, the energy score of the peptide with different PD-related targets was also computed (Table 2), and the figures of the interactions are shown in Fig. 4.

The TVTAMNVVYALK neuroavailable peptide has a molecular weight of around 1.30 kDa, an α -helix structure, low water solubility, and high hydrophobicity, suggesting that the amino acid sequence, low molecular weight, and helical secondary structure could favor the absorption of the peptide despite not having a high hydrophobicity. According to PreTP-Stack, it might possess high therapeutic potential (>0.5), and the PreAIP tool also provided an adequate result of anti-inflammatory potential of the peptide, showing a value which in other studies have been reported for peptides exhibiting *in vitro* activity.⁵³

The *in silico* antioxidant properties (quantified by FRS and CHEL scores) showed that TVTAMNVVYALK could exert antioxidant activity, as the values were high as values in other peptides demonstrating *in vitro* activity.⁵⁴ On top of that, the SCMB3PP tool was used to predict whether the peptide could




Table 1 Characterization of the 20 peptides with the highest Pre-AIP score identified in the neuroHPH60A + 15F based on *in silico* analyses, and TVTAMNVVYALK, a neuroavailable peptide

Peptide	PreAIP ^a	PeptideRanker (threshold 0.5) ^b	PreTP-Stack- anti- inflammatory (threshold 0.5) ^c	AnoxPred (FRS) ^d	SCMB3PP (threshold (CHEL) ^d 749) ^e	Hydrophobicity ^f	Steric hindrance ^f	Water solubility ^f	Charge ^f	Amphiphaticity ^f	Self- aggregation- prone region & amyloids ^g	Disorder Probability (%) ^g	α-Helix ^g	β-Strand ^g	Coil ^g		
SLGGGTSGMASLLSK	0.682	0.688	0.618	0.410	0.214	779.50	0.07	0.60	Poor	9.11	1	0.22	4-7 (NI)	100	33.3	—	66.7
LLSNASCTINCLAPLAK	0.624	0.510	0.672	0.450	0.201	792.25	0.06	0.61	Poor	9.11	1	0.22	5-8 (NI)	100	—	—	100
IWYGFQNALLAAL	0.617	0.362	0.572	0.330	0.213	785.06	-0.02	0.56	Poor	8.38	1	0.22	6-9 (NI)	100	—	10.0	90.0
DSTLIMQGLIV	0.606	0.606	0.500	0.406	0.211	753.75	0.21	0.59	Poor	5.88	0	0.11	4-8 (PA)	100	—	55.6	44.4
LDADEALAVNLYVEGS	0.595	0.352	0.566	0.333	0.277	768.20	0.11	0.62	Poor	3.80	-1	0.11	6-9 (NI)	100	—	—	100
AAAQLGSVTEQLQACK	0.588	0.389	0.579	0.357	0.171	738.93	0.05	0.63	Good	3.44	-4	0.16	5-9 (NI)	100	40.0	—	60.0
ADLGGGNISLAK	0.588	0.385	0.524	0.373	0.214	766.27	-0.06	0.59	Poor	6.32	0	0.46	5-8 (NI)	100	—	55.6	44.4
VNRAAMTLPIL	0.584	0.466	0.642	0.373	0.222	762.25	0.04	0.6	Poor	6.19	0	0.28	1-6 (NI)	100	60.0	—	40.0
WLNNGNRTPLVL	0.579	0.426	0.628	0.436	0.181	648.67	0.00	0.59	Poor	10.11	1	0.25	3-9 (NI)	100	—	55.6	44.4
FEQLCSDRLL	0.573	0.749	0.566	0.356	0.227	799.82	-0.05	0.61	Poor	9.10	1	0.20	4-9 (NI)	100	54.6	—	45.4
AVRLPHWNLN	0.573	0.551	0.535	0.585	0.256	770.89	-0.17	0.64	Good	4.38	-1	0.50	6-9 (NI)	100	—	—	100
LDTELLITVGD	0.571	0.077	0.507	0.336	0.241	789.11	-0.13	0.53	Poor	10.11	1.5	0.39	8-12 (NI)	100	81.2	—	18.8
LLNEPTAAALGNFMLL	0.568	0.766	0.554	0.319	0.243	767.90	0.04	0.61	Good	3.50	-3	0.12	10-13 (NI)	100	—	—	100
LLGENAHALIQKV	0.550	0.131	0.551	0.486	0.265	757.33	0.14	0.59	Poor	4.00	-1	0.08	1-4 (NI)	100	40.0	—	60.0
LEVLELMIDTR	0.548	0.111	0.548	0.333	0.2145	779.75	-0.17	0.58	Good	5.41	-0.5	0.69	6-9 (PA)	100	—	50.0	50.0
SYELPQGVLTLLNDN	0.547	0.282	0.467	0.347	0.173	775.22	-0.15	0.64	Good	4.14	-2	0.50	8-11 (NI)	100	—	—	100
JHFFAAHLL	0.546	0.729	0.584	0.477	0.296	778.33	-0.10	0.63	Poor	3.67	-2	0.16	5-8 (NI)	100	—	—	100
KNEQLYQPLLSK	0.542	0.176	0.554	0.351	0.232	793.75	0.20	0.41	Poor	7.26	1	0.32	5-8 (NI)	100	—	—	100
VLLGGGNPLTLEAGFR	0.542	0.509	0.604	0.437	0.205	780.82	-0.25	0.61	Good	8.94	1	0.93	1-6 (NI)	100	—	—	100
TVTAMNVVYALK	0.449	0.081	0.566	0.386	0.194	792.00	0.06	0.61	Poor	6.36	0	0.23	1-6 (NI)	100	—	—	100
						701.82	0.07	0.64	Poor	8.94	1	0.31	1-4 (NI)	100	—	18.2	81.8

^a PreAIP: peptides were subjected to calculations via <https://kurata14.bio.kyutech.ac.jp/PreAIP/>, where the probability of the peptides to exert anti-inflammatory effects was estimated based on different types of features including primary sequence, evolutionary and structural information through a random forest classifier (threshold to be considered highly anti-inflammatory >0.468). ^b PeptideRanker: the likelihood of the peptides being bioactive was evaluated by PeptideRanker (<https://bioware.ucd.ie/~compass/biowareweb/>), a server to predict bioactive peptides based on a novel N-to-1 neural network, by giving scores ranging from 0 to 1. A higher score indicates a greater likelihood of the peptide being bioactive. ^c PreTP-Stack: the anti-inflammatory potential of the peptides was also estimated with PreTP-Stack (<https://blulab.net/PreTP-Stack/>), which is based on stacked ensemble learning, by giving scores ranging from 0 to 1. A higher score indicates a greater likelihood of the peptide being anti-inflammatory. ^d AnOrPePpred tool (<https://services.bioninformatics.dtu.dk/service.php?AnOrPePpred-1.0>) uses deep learning to predict the anti-oxidant properties (quantified by free radical scavenging and ion chelating scores) of peptides by giving scores ranging from 0 to 1. ^e SCMB3PP: it allows for the prediction and characterization of blood-brain barrier penetrating peptides using estimated propensity scores of dipeptides, and the server available here: <https://protein.bio.unipd.it/pasta2/>. The web server PASTA 2.0 (<https://proteinanywhere.com/SCMB3PP/>) physico-chemical characterization was estimated with ToxinPred: via <https://webs.iitd.edu.in/raghava/toxinpred/design.php/>. ^f The web server PASTA 2.0 (<https://protein.bio.unipd.it/pasta2/>) was implicated to compute the tendency of peptide self-aggregation specific to the possible region at the sequence (with the recorded number starting from the N-terminus). For peptide discrimination, the optimal thresholds were switched as top = 1 and energy <-5 PEU (1 PEU (Pasta Energy Unit) = 1.192 kcal mol⁻¹). ^g NI: no amyloid predicted; PA: parallel aggregation computed. The probability of intrinsic disorder and the portion of estimated secondary structure that complements the aggregation data were also reported.

Table 2 Molecular docking results for the receptor-peptide binding including the affinity of TVTAMNVVYALK with the target receptors, the cluster size, and the interaction (position, type, and distance)

Docking results					
Possible best results					
Receptor	Affinity (kcal mol ⁻¹)	Cluster size	Interactions		
			Interaction of amino acid residues	Bond distance (Å)	Type of interaction bond
α-Synuclein	-11.6	37	Thr1 - Gly73 Thr3 - Gly73 Ala4 - Val77 Ala4 - Lys80 Val8 - Val74 Leu11 - Val70 Leu11 - Val74 Lys12 - Val71	2.20 2.73 3.83 4.82 5.34 4.62 3.95 3.95	Carbon hydrogen Carbon hydrogen Alkyl Alkyl Alkyl Alkyl Alkyl Alkyl
COMT	-16.6	75	Thr1 - Glu37 Ala10 - Trp143 Lys12 - Met40	3.98 3.43 3.92	Attractive charge Pi-sigma Alkyl
MAO-B	-15.3	37	Val2 - Gln416 Val2 - Arg412 Thr3 - Arg412 Thr3 - Arg354 Ala4 - Arg412 Ala4 - Val413 Ala4 - Met281 Ala4 - Met281 Val7 - Ala353 Tyr9 - Glu390 Leu11 - Leu56 Leu11 - Lys386 Lys12 - Leu46	4.13 3.44 2.00 2.10 3.48 3.24 4.57 2.95 2.25 2.73 4.89 4.58 4.99	Unfavorable bump Alkyl Carbon hydrogen Conventional hydrogen Alkyl Unfavorable bump Alkyl Unfavorable bump Conventional hydrogen Conventional hydrogen Alkyl Alkyl Alkyl

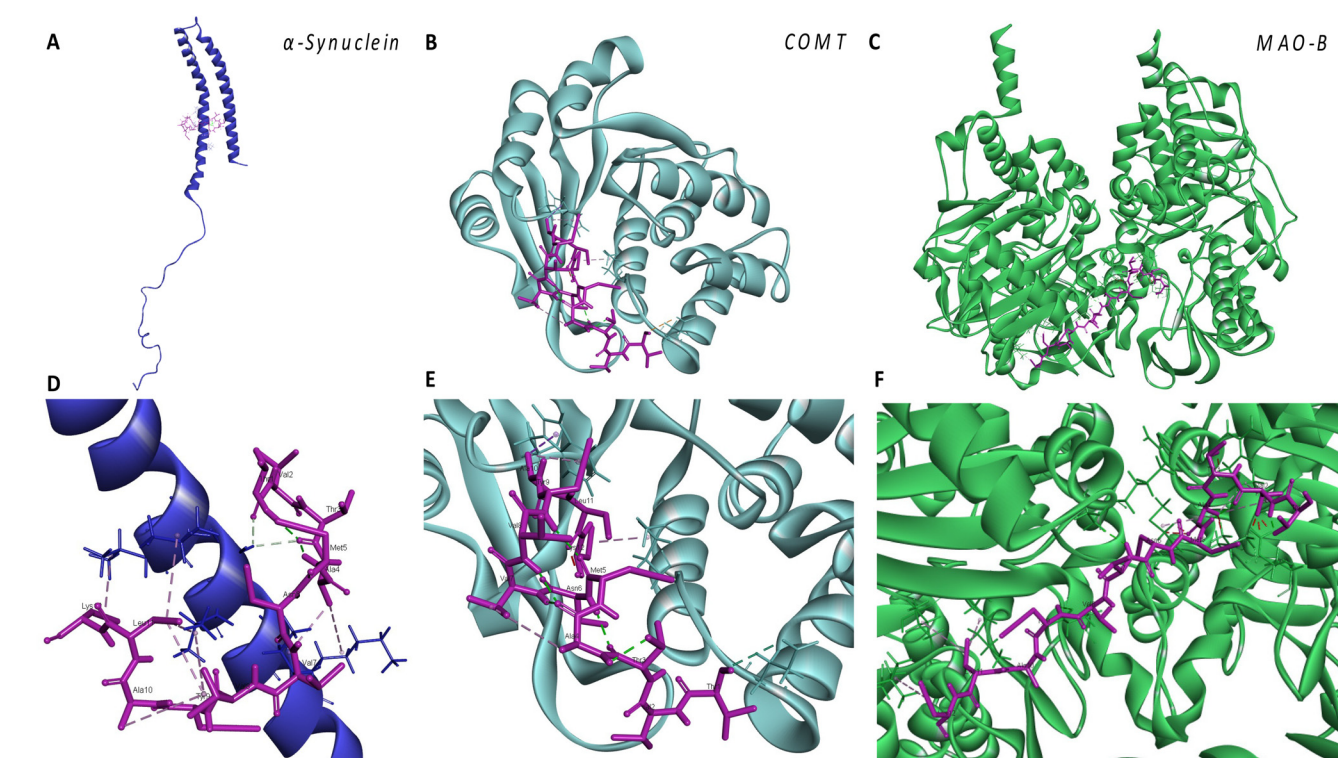


Fig. 4 Visualization of the receptor-peptide complex using a Biovia Discovery Studio Visualizer. (A) α-Synuclein-TVTAMNVVYALK binding sites and their interactions; (B) COMT-TVTAMNVVYALK binding sites and their interactions; (C) MAO-B-TVTAMNVVYALK binding sites and their interactions. (D) TTVTAMNVVYALK interactions with the atoms involved in the pocket-binding site of α-synuclein; (E) TTVTAMNVVYALK interactions with the atoms involved in the pocket-binding site of COMT; and (F) TTVTAMNVVYALK interactions with the atoms involved in the pocket-binding site of MAO-B.



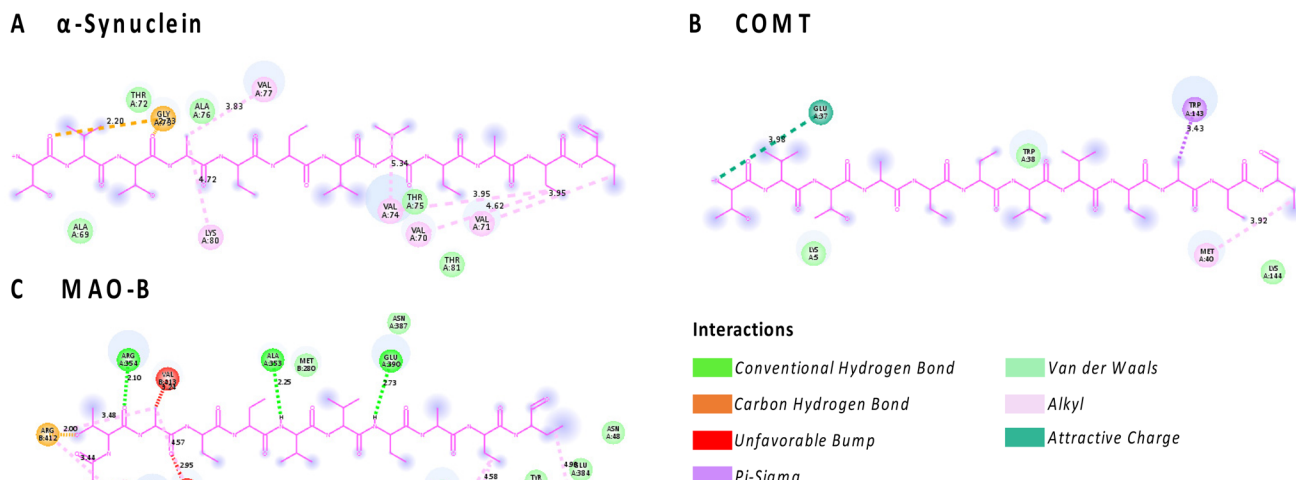


Fig. 5 2D residue diagram analysis for TVTAMNVVYALK with its respective interaction bonds with the receptors (A) α -synuclein, (B) COMT, and (C) MAO-B visualized using a Bovia Discovery Studio Visualizer

penetrate the BBB, and a value of 701.8 was obtained, not reaching the threshold indicated by the authors. However, as this peptide was identified in the neuroHPH60A + 15F, this highlights that, even promising, these tools should not be used to do statements on the bioactivity or bioavailability of peptides. It must be noted that these *in silico* tools have both advantages and limitations,⁵² and the results obtained from them cannot be used exclusively as evidence to state that a peptide is exerting specific bioactivities. For this reason, *in vitro* and *in vivo* validation are needed in order to suggest the potential properties of these peptides.

There is scarce information about identified food-derived peptides targeting PD-related molecules. In the inhibition of MAO, for instance, whose relevance is based on the fact that are essential deamination enzymes for neurotransmitters and other amines; a recent study identified MAO inhibitory peptides from soybean protein hydrolysate through ultrafiltration purification and *in silico* prediction. The most promising sequences were YSPYPQ, which exerted an inhibitory activity against MAO-A with an IC_{50} of 0.663 mM, while PLYSN possessed the strongest MAO-B inhibition effect with an IC_{50} of 0.204 mM. Similar to our results, molecular docking revealed the affinity of the peptides for the enzymes, leading to potentially obstructing the admission of the substrates to the active sites.⁵⁵ Similarly, the presence of Trp, Gly, and Leu residues in peptides might contribute to the anti-inflammation according to Wang *et al.* (2020).⁴⁵ To the author's knowledge, little *in vivo* studies have been published in the field of food-derived peptides. For instance, an analysis of the efficacy of brain protein hydrolysate injections in the treatment of elderly patients with PD was reported by Liu *et al.* (2017).⁵⁶

Finally, the molecular docking analyses of the neuroavailable peptide found in all the fractions (TVTAMNVVYALK) with different receptors showed the high potential of this peptide to

interact with them. The affinities of the sequences with α -syn, COMT, and MAO-B were -11.6 , -16.6 , and -15.3 kcal mol $^{-1}$ respectively, which are values indicating that the complex is stable and consequently the target compounds' activity might be compromised. The graphical representation of the interaction of the peptide with the different receptors is shown in Fig. 5, where it is observed the numerous interactions of diverse nature established between the different residues, offering stability to the complex. To the author's knowledge, the peptide identified hereby stemming from a HPH has not been identified previously. Hempseed bioactive oligopeptides have shown their ability to modify the inflammatory response in multiple ways to regulate physiological processes such as the development of PD. Further investigations and human studies are needed to corroborate these results.

Conclusions

HPHs have shown potential to act as anti-inflammatory agents in several *in vitro* assays. The present work provides a novel study on the effect of HPH60A + 15F administered to LRRK2 transgenic mice to evaluate its implications in inflammation and neuroprotection in PD. It has been reported that acute treatment with HPH60A + 15F (10 mg kg⁻¹ day⁻¹) administered orally through an esophageal tube for 7 days to 18-month-old LRRK2 mice decreases α -syn, CD68, iNOS, and COX2 protein aggregates in the brain. The treatment significantly decreases TNF- α gene expression levels in the striatum area of the brain. The results indicate a statistically significant decrease in the gene expression of some additional pro-inflammatory cytokines in BMDMs. Therefore, these studies suggest that HPH60A + 15F may be able to reduce neuroinflammation by decreasing cytokine gene expression in the brain, which could

show promise for PD. To conclude whether this hydrolysate could also have anti-inflammatory effects acting at other levels, further studies are required. On top of that, the peptidome of the neuroavailable fraction was identified, and 182 unique sequences were characterized employing *in silico* tools to define their physicochemical properties and bioactivity. The results considering the neuroavailable sample indicate that most of the peptides in the sample contribute to the bioactivity reported in the *in vivo* studies. In addition to that, one peptide (TVTAMNVVYALK) was identified in the original HPH60A + 15F, the bioHPH60A + 15F, and neuroHPH60A + 15F, indicating its potential to be used as a therapeutic agent, reaching the brain. This study shows the prospective role that hemp-seed-derived oligopeptides obtained with alcalase and flavourzyme might have in neuromodulation, with a high likelihood of preventing the development of diseases such as PD.

Author contributions

Conceptualization, M. C. M.-L., S. M.-d. I. P., and C. M. C.; methodology, M. T.-L. and P. T.; formal analysis, M. T.-L. and T. G.-d. I. R.; investigation, A. V. and R. T.-S.; resources, S. M.-d. I. P. and M. C. M.-L.; writing—original draft preparation, F. R.-P. and C. M. C.; writing—review and editing, S. M.-d. I. P.; supervision, M. C. M.-L. and C. M.-C.; funding acquisition, S. M.-d. I. P. and M. C. M.-L. All authors have read and agreed to the published version of the manuscript.

Data availability

The data supporting this article have been included as part of the ESI.†

Conflicts of interest

The authors declare that they have no known competing financial interests or personal relationships that could have appeared to influence the work reported in this paper.

Acknowledgements

This research was funded by grant P20_00661 from the Andalusian Plan for Research, Development and Innovation (PAIDI) 2020 and by grant US-1381492 from the European Regional Development Fund (ERDF). Maria Torrecillas-Lopez has the benefit of a doctoral fellowship from the Spanish Ministry of Science, Innovation, and Universities (PREP2022-000408). F. R.-P. has the benefit of a Juan de la Cierva postdoctoral fellowship (FJC2022-050043-I) from the Spanish Ministry of Science and Innovation. R. T.-S. has the benefit of a “Margarita Salas” postdoctoral grant from the Recovery, Transformation and Resilience Plan (Next Generation EU). Teresa Gonzalez-de la Rosa acknowledges her contract sup-

ported by the “Programa Investigo” funded by the European Union–Next Generation EU (C23.I1.P03.S01.01). The authors thank Carlos Fuentes from the Proteomics Unit of the Central Research Support Service of Cordoba University (UCO) for his technical assistance during the fulfilment of this work.

References

- 1 M. Ahmad, S. Qureshi, M. H. Akbar, S. A. Siddiqui, A. Gani, M. Mushtaq, *et al.*, Plant-based meat alternatives: Compositional analysis, current development and challenges, *Appl. Food Res.*, 2022, **2**(2), 100154, DOI: [10.1016/j.afres.2022.100154](https://doi.org/10.1016/j.afres.2022.100154).
- 2 F. Alfieri, F. Rivero-Pino, P. Zakidou, A. Fernandez-Dumont and R. Roldán-Torres, Processes for obtaining plant-based dairy and meat substitutes, in *Sustainable Food Science - A Comprehensive Approach*, Elsevier, 2023, pp. 75–99. DOI: [10.1016/b978-0-12-823960-5.00051-2](https://doi.org/10.1016/b978-0-12-823960-5.00051-2).
- 3 F. Rivero-Pino, M. C. Millan-Linares and S. Montserrat-De la Paz, Hemp protein, in *Sustainable Food Science: A Comprehensive Approach*, Elsevier, 2023. DOI: [10.1016/B978-0-12-823960-5.00014-7](https://doi.org/10.1016/B978-0-12-823960-5.00014-7).
- 4 A. Jurgonski, P. M. Opyd and B. Fotschki, Effects of native or partially defatted hemp seeds on hindgut function, antioxidant status and lipid metabolism in diet-induced obese rats, *J. Funct. Foods*, 2020, **72**, 104071, DOI: [10.1016/j.jff.2020.104071](https://doi.org/10.1016/j.jff.2020.104071).
- 5 R. C. Mollard, A. Johnston, A. S. Leon, H. Wang, P. J. Jones and D. S. Mackay, Acute effects of hemp protein consumption on glycemic and satiety control: results of 2 randomized crossover trials, *Appl. Physiol., Nutr., Metab.*, 2021, **46**, 887–896, DOI: [10.1139/apnm-2020-0907](https://doi.org/10.1139/apnm-2020-0907).
- 6 G. Rizzo, M. A. Storz and G. Calapai, The role of hemp (*Cannabis sativa L.*) as a functional food in vegetarian nutrition, *Foods*, 2023, **12**, 3505, DOI: [10.3390/foods12183505](https://doi.org/10.3390/foods12183505).
- 7 F. Rivero-Pino, Bioactive food-derived peptides for functional nutrition: Effect of fortification, processing and storage on peptide stability and bioactivity within food matrices, *Food Chem.*, 2023, **406**, 135046, DOI: [10.1016/j.foodchem.2022.135046](https://doi.org/10.1016/j.foodchem.2022.135046).
- 8 S. Montserrat-De la Paz, F. Rivero-Pino, A. Villanueva, R. Toscano-Sánchez, M. E. Martín, F. Millán, *et al.*, Nutritional composition, ultrastructural characterization, and peptidome profile of antioxidant hemp protein hydrolysates, *Food Biosci.*, 2023, **53**, 102561, DOI: [10.1016/j.fbio.2023.102561](https://doi.org/10.1016/j.fbio.2023.102561).
- 9 M. C. Millan-Linares, F. Rivero-Pino, T. Gonzalez-de la Rosa, A. Villanueva and S. Montserrat-de la Paz, Identification, characterization, and molecular docking of immunomodulatory oligopeptides from bioavailable hemp-seed protein hydrolysates, *Food Res. Int.*, 2024, **176**, 113712, DOI: [10.1016/j.foodres.2023.113712](https://doi.org/10.1016/j.foodres.2023.113712).
- 10 S. Montserrat-De la Paz, A. Villanueva-Lazo, F. Millán, V. Martín-Santiago, F. Rivero-Pino and M. C. Millan-



Linares, Production and identification of immunomodulatory peptides in intestine cells obtained from hemp industrial by-products, *Food Res. Int.*, 2023, **174**, 113616, DOI: [10.1016/j.foodres.2023.113616](https://doi.org/10.1016/j.foodres.2023.113616).

11 S. Montserrat-De la Paz, G. Carrillo-Berdasco, F. Rivero-Pino, A. Villanueva-Lazo and M. C. Millan-Linares, Hemp protein hydrolysates modulate inflammasome-related genes in microglial cells, *Biology*, 2023, **12**, 49, DOI: [10.3390/biology12010049](https://doi.org/10.3390/biology12010049).

12 N. M. Rodriguez-Martin, S. Montserrat-De la Paz, R. Toscano, E. Grao-Cruces, A. Villanueva, J. Pedroche, *et al.*, Hemp (*Cannabis sativa L.*) protein hydrolysates promote anti-inflammatory response in primary human monocytes, *Biomolecules*, 2020, **10**, 803, DOI: [10.3390/biom10050803](https://doi.org/10.3390/biom10050803).

13 X. S. Zeng, W. S. Geng, J. J. Jia, L. Chen and P. P. Zhang, Cellular and molecular basis of neurodegeneration in Parkinson disease, *Front. Aging Neurosci.*, 2018, **10**, 1–16, DOI: [10.3389/fnagi.2018.00109](https://doi.org/10.3389/fnagi.2018.00109).

14 C. Ren, Y. Ding, S. Wei, L. Guan, C. Zhang, Y. Ji, *et al.*, G2019S Variation in LRRK2: An Ideal Model for the Study of Parkinson's Disease?, *Front. Hum. Neurosci.*, 2019, **13**, 306, DOI: [10.3389/fnhum.2019.00306](https://doi.org/10.3389/fnhum.2019.00306).

15 M. Yue, K. M. Hinkle, P. Davies, E. Trushina, F. C. Fiesel, T. A. Christenson, *et al.*, Progressive dopaminergic alterations and mitochondrial abnormalities in LRRK2 G2019S knock-in mice, *Neurobiol. Dis.*, 2015, **78**, 172–195, DOI: [10.1016/j.nbd.2015.02.031](https://doi.org/10.1016/j.nbd.2015.02.031).

16 A. J. Lees, J. Hardy and T. Revesz, Parkinson's disease, *Lancet*, 2009, **373**(9680), 2055–2066, DOI: [10.1016/S0140-6736\(09\)60492-X](https://doi.org/10.1016/S0140-6736(09)60492-X).

17 G. Bieri, M. Brahic, L. Bousset, J. Couthouis, N. J. Kramer, R. Ma, *et al.*, LRRK2 modifies α -syn pathology and spread in mouse models and human neurons, *Acta Neuropathol.*, 2019, **137**(6), 961–980, DOI: [10.1007/s00401-019-01995-0](https://doi.org/10.1007/s00401-019-01995-0).

18 N. Panicker, P. Ge, V. L. Dawson and T. M. Dawson, The cell biology of Parkinson's disease, *J. Cell Biol.*, 2021, **220**(4), 1–31, DOI: [10.1083/jcb.202012095](https://doi.org/10.1083/jcb.202012095).

19 E. Lazdon, N. Stolero and D. Frenkel, Microglia and Parkinson's disease: footprints to pathology, *J. Neural Transm.*, 2020, **127**(2), 149–158, DOI: [10.1007/s00702-020-02154-6](https://doi.org/10.1007/s00702-020-02154-6).

20 P. J. Patil, S. S. Sutar, M. Usman, D. N. Patil, M. J. Dhanavade, Q. Shehzad, *et al.*, Exploring bioactive peptides as potential therapeutic and biotechnology treasures: A contemporary perspective, *Life Sci.*, 2022, **301**, 120637, DOI: [10.1016/j.lfs.2022.120637](https://doi.org/10.1016/j.lfs.2022.120637).

21 K. B. J. Franklin and G. Paxinos, *The Mouse Brain in Stereotaxic Coordinates*, Academic Press, 2008.

22 S. Montserrat-De la Paz, M. C. Naranjo, S. Lopez, R. Abia, F. J. G. Muriana and B. Bermúdez, Niacin and its metabolites as master regulators of macrophage activation, *J. Nutr. Biochem.*, 2017, **39**, 40–47, DOI: [10.1016/j.jnutbio.2016.09.008](https://doi.org/10.1016/j.jnutbio.2016.09.008).

23 S. Gupta, P. Kapoor, K. Chaudhary, A. Gautam, R. Kumar and G. P. S. Raghava, In silico approach for predicting toxicity of peptides and proteins, *PLoS One*, 2013, **8**, e73957, DOI: [10.1371/journal.pone.0073957](https://doi.org/10.1371/journal.pone.0073957).

24 T. H. Olsen, B. Yesiltas, F. I. Marin, M. Pertseva, P. J. García-Moreno, S. Gregersen, *et al.*, AnOxPePred: using deep learning for the prediction of antioxidative properties of peptides, *Sci. Rep.*, 2020, **10**(1), 1–10, DOI: [10.1038/s41598-020-78319-w](https://doi.org/10.1038/s41598-020-78319-w).

25 M. S. Khatun, M. M. Hasan and H. Kurata, PreAIP: Computational prediction of anti-inflammatory peptides by integrating multiple complementary features, *Front. Genet.*, 2019, **10**, 129, DOI: [10.3389/fgene.2019.00129](https://doi.org/10.3389/fgene.2019.00129).

26 K. Yan, H. Lv, J. Wen, Y. Guo, Y. Xu and B. Liu, PreTP-Stack: Prediction of therapeutic peptides based on the stacked ensemble learning, *IEEE/ACM Trans. Comput. Biol. Bioinf.*, 2023, **20**(2), 1337–1344, DOI: [10.1109/TCBB.2022.3183018](https://doi.org/10.1109/TCBB.2022.3183018).

27 P. Charoenkwan, P. Chumnanpuen, N. Schaduangrat, P. Lio', M. A. Moni and W. Shoombuatong, Improved prediction and characterization of blood-brain barrier penetrating peptides using estimated propensity scores of dipeptides, *J. Comput. Aided Mol. Des.*, 2022, **36**(11), 781–796, DOI: [10.1007/s10822-022-00476-z](https://doi.org/10.1007/s10822-022-00476-z).

28 C. Mooney, N. J. Haslam, G. Pollastri and D. C. Shields, Towards the improved discovery and design of functional peptides: Common features of diverse classes permit generalized prediction of bioactivity, *PLoS One*, 2012, **7**, e45012, DOI: [10.1371/journal.pone.0045012](https://doi.org/10.1371/journal.pone.0045012).

29 E. Janda, L. Boi and A. R. Carta, Microglial phagocytosis and its regulation: A therapeutic target in Parkinson's disease?, *Front. Mol. Neurosci.*, 2018, **11**, 144, DOI: [10.3389/fnmol.2018.00144](https://doi.org/10.3389/fnmol.2018.00144).

30 X. Ma, J. Li, X. Cui, C. Li and Z. Wang, Dietary supplementation with peptides from sesame cake alleviates Parkinson's associated pathologies in *Caenorhabditis elegans*, *J. Funct. Foods*, 2020, **65**, 103737, DOI: [10.1016/j.jff.2019.103737](https://doi.org/10.1016/j.jff.2019.103737).

31 E. Croisier, L. B. Moran, D. T. Dexter, R. K. B. Pearce and M. B. Graeber, Microglial inflammation in the parkinsonian substantia nigra: relationship to alpha-synuclein deposition, *J. Neuroinflammation*, 2005, **2**(1), 14, DOI: [10.1186/1742-2094-2-14](https://doi.org/10.1186/1742-2094-2-14).

32 D. A. Chistiakov, M. C. Killingsworth, V. A. Myasoedova, A. N. Orekhov and Y. V. Bobryshev, CD68/macrosialin: Not just a histochemical marker, *Lab. Invest.*, 2017, **97**(1), 4–13, DOI: [10.1038/labinvest.2016.116](https://doi.org/10.1038/labinvest.2016.116).

33 R. A. Velliquette, D. J. Fast, E. R. Maly, A. M. Alashi and R. E. Aluko, Enzymatically derived sunflower protein hydrolysate and peptides inhibit NF κ B and promote monocyte differentiation to a dendritic cell phenotype, *Food Chem.*, 2020, **319**, 126563, DOI: [10.1016/j.foodchem.2020.126563](https://doi.org/10.1016/j.foodchem.2020.126563).

34 V. Chiurchiù, A. Leuti and M. Maccarrone, Cannabinoid signaling and neuroinflammatory diseases: A melting pot for the regulation of brain immune responses, *J. Neuroimmune Pharmacol.*, 2015, **10**(2), 268–280, DOI: [10.1007/s11481-015-9584-2](https://doi.org/10.1007/s11481-015-9584-2).



35 M. A. Cinelli, H. T. Do, G. P. Miley and R. B. Silverman, Inducible nitric oxide synthase: Regulation, structure, and inhibition, *Med. Res. Rev.*, 2020, **40**(1), 158–189, DOI: [10.1002/med.21599](https://doi.org/10.1002/med.21599).

36 A. Sierra, J. Navascués, M. A. Cuadros, R. Calvente, D. Martín-Oliva, R. M. Ferrer-Martín, *et al.*, Expression of inducible nitric oxide synthase (iNOS) in microglia of the developing quail retina, *PLoS One*, 2014, **9**, e106048, DOI: [10.1371/journal.pone.0106048](https://doi.org/10.1371/journal.pone.0106048).

37 X. Wang and E. K. Michaelis, Selective neuronal vulnerability to oxidative stress in the brain, *Front. Aging Neurosci.*, 2010, **2**, 1–13, DOI: [10.3389/fnagi.2010.00012](https://doi.org/10.3389/fnagi.2010.00012).

38 D. E. López and S. J. Ballaz, The role of brain cyclooxygenase-2 (Cox-2) beyond neuroinflammation: neuronal homeostasis in memory and anxiety, *Mol. Neurobiol.*, 2020, **57**(12), 5167–5176, DOI: [10.1007/s12035-020-02087-x](https://doi.org/10.1007/s12035-020-02087-x).

39 A. Rauf, H. Badoni, T. Abu-Izneid, A. Olatunde, M. M. Rahman, S. Painuli, *et al.*, Neuroinflammatory markers: Key indicators in the pathology of neurodegenerative diseases, *Molecules*, 2022, **27**(10), 1–25, DOI: [10.3390/molecules27103194](https://doi.org/10.3390/molecules27103194).

40 Q. Liang, X. Ren, M. Chalamaiyah and H. Ma, Simulated gastrointestinal digests of corn protein hydrolysate alleviate inflammation in caco-2 cells and a mouse model of colitis, *J. Food Sci. Technol.*, 2020, **57**(6), 2079–2088, DOI: [10.1007/s13197-020-04242-7](https://doi.org/10.1007/s13197-020-04242-7).

41 J. Le Faouder, B. Arnaud, R. Lavigne, C. Lucas, E. Com, E. Bouvret, *et al.*, Fish hydrolysate supplementation prevents stress-induced dysregulation of hippocampal proteins relative to mitochondrial metabolism and the neuronal network in mice, *Foods*, 2022, **11**, 1591, DOI: [10.3390/foods11111591](https://doi.org/10.3390/foods11111591).

42 J. Maroon and J. Bost, Review of the neurological benefits of phytocannabinoids, *Surg. Neurol. Int.*, 2018, **9**, 91, DOI: [10.4103/SNLSNLI_45_18](https://doi.org/10.4103/SNLSNLI_45_18).

43 I. Russo, L. Bubacco and E. Greggio, LRRK2 and neuroinflammation: Partners in crime in Parkinson's disease?, *J. Neuroinflammation*, 2014, **11**, 52, DOI: [10.1186/1742-2094-11-52](https://doi.org/10.1186/1742-2094-11-52).

44 J. Ji, X. Yi, Y. Zhu, H. Yu, S. Huang, Z. Liu, *et al.*, Tilapia head protein hydrolysate attenuates scopolamine-induced cognitive impairment through the gut-brain axis in mice, *Foods*, 2021, **10**, 3129, DOI: [10.3390/foods10123129](https://doi.org/10.3390/foods10123129).

45 S. Wang, L. Zheng, T. Zhao, Q. Zhang, Y. Liu, B. Sun, *et al.*, Inhibitory effects of walnut (*Juglans regia*) peptides on neuroinflammation and oxidative stress in lipopolysaccharide-induced cognitive impairment mice, *J. Agric. Food Chem.*, 2020, **68**(8), 2381–2392, DOI: [10.1021/acs.jafc.9b07670](https://doi.org/10.1021/acs.jafc.9b07670).

46 S. Wang, G. Su, X. Zhang, G. Song, L. Zhang, L. Zheng, *et al.*, Characterization and exploration of potential neuroprotective peptides in walnut (*Juglans regia*) protein hydrolysate against cholinergic system damage and oxidative stress in scopolamine-induced cognitive and memory impairment mice and zebrafish, *J. Agric. Food Chem.*, 2021, **69**(9), 2773–2783, DOI: [10.1021/acs.jafc.0c07798](https://doi.org/10.1021/acs.jafc.0c07798).

47 F. Patricio, A. A. Morales-Andrade, A. Patricio-Martínez and I. D. Limón, Cannabidiol as a therapeutic target: Evidence of its neuroprotective and neuromodulatory function in Parkinson's disease, *Front. Pharmacol.*, 2020, **11**, 1–24, DOI: [10.3389/fphar.2020.595635](https://doi.org/10.3389/fphar.2020.595635).

48 A. Tanaka, J. To, B. O'Brien, S. Donnelly and M. Lund, Selection of reliable reference genes for the normalisation of gene expression levels following time course LPS stimulation of murine bone marrow derived macrophages, *BMC Immunol.*, 2017, **18**(1), 1–12, DOI: [10.1186/s12865-017-0223-y](https://doi.org/10.1186/s12865-017-0223-y).

49 R. S. Kaushik, J. E. Uzonna, Y. Zhang, J. R. Gordon and H. Tabel, Innate resistance to experimental African trypanosomiasis: Differences in cytokine (TNF- α , IL-6, IL-10 and IL-12) production by bone marrow-derived macrophages from resistant and susceptible mice, *Cytokine*, 2000, **12**(7), 1024–1034, DOI: [10.1006/cyto.2000.0685](https://doi.org/10.1006/cyto.2000.0685).

50 L. Soriano-Romani, J. A. Nieto and S. García-Benlloch, Immunomodulatory role of edible bone collagen peptides on macrophage and lymphocyte cell cultures, *Food Agric. Immunol.*, 2022, **33**(1), 546–562, DOI: [10.1080/09540105.2022.2098936](https://doi.org/10.1080/09540105.2022.2098936).

51 S. Caira, G. Picariello, G. Renzone, S. Arena, A. D. Troise, S. De Pascale, *et al.*, Recent developments in peptidomics for the quali-quantitative analysis of food-derived peptides in human body fluids and tissues, *Trends Food Sci. Technol.*, 2022, **126**, 41–60, DOI: [10.1016/j.tifs.2022.06.014](https://doi.org/10.1016/j.tifs.2022.06.014).

52 F. Rivero-Pino, M. C. Millan-Linares and S. Montserrat-De la Paz, Strengths and limitations of in silico tools to assess physicochemical properties, bioactivity, and bioavailability of food-derived peptides, *Trends Food Sci. Technol.*, 2023, **138**, 433–440, DOI: [10.1016/j.tifs.2023.06.023](https://doi.org/10.1016/j.tifs.2023.06.023).

53 J. Rivera-Jiménez, C. Berraquero-García, R. Pérez-Gálvez, P. J. Pérez-Gálvez, F. J. Espejo-Carpio, A. Guadix, *et al.*, Peptides and protein hydrolysates exhibiting anti-inflammatory activity: Sources, structural features and modulation mechanisms, *Food Funct.*, 2022, **13**, 12510–12540, DOI: [10.1039/d2fo02223k](https://doi.org/10.1039/d2fo02223k).

54 Z. Guo, Y. Yang, B. Hu, L. Zhu, C. Liu, M. Li, *et al.*, The bioaccessibility of yak bone collagen hydrolysates: Focus on analyzing the variation regular of peptides and free amino acids, *Foods*, 2023, **12**, 1003, DOI: [10.3390/foods12051003](https://doi.org/10.3390/foods12051003).

55 F. Ying, S. Lin, J. Li, X. Zhang and G. Chen, Identification of monoamine oxidases inhibitory peptides from soybean protein hydrolysate through ultrafiltration purification and in silico studies, *Food Biosci.*, 2021, **44**(PA), 101355, DOI: [10.1016/j.fbio.2021.101355](https://doi.org/10.1016/j.fbio.2021.101355).

56 W. Liu, J. Li, Y. Peng, L. Liu, J. Shen and J. Xu, Analysis of the efficacy of brain protein hydrolysate injection in the treatment of elderly patients with Parkinson, *Prog. Mod. Biomed.*, 2017, **24**, 5312–5314.

